

Università degli Studi di Padova

Dipartimento di Tecnica e Gestione dei Sistemi Industriali

Product Innovation Engineering degree

---

**Optimization of the sensor support prototype for the alignment of  
components in the High Luminosity LHC**

---

Academic Year 2021-2022

Christian CASAROTTO

CERN supervisor: Andreas HERTY Dipl.-Ing. (FH) MPhil

UNIPD supervisors: Dr. Lisa BIASETTO

& Dr. Emanuele SARTORI

---

## **Acknowledgements**

*I would like to thank my CERN supervisor, M. Andreas Herty, for his guidance through the development and literature review of this thesis. The assistance he provided me to tackle new fields was invaluable for the development of my work and thesis whilst at CERN. I would also like to extend my gratitude to my UNIPD professors, Dr. Biasetto Lisa and Dr. Sartori Emanuele, for supervising my thesis work and taking part in this project.*

---

# Contents

<b>1 CERN</b>	<b>3</b>
1.1 Organization . . . . .	3
1.2 Particle accelerators . . . . .	3
1.3 Large Hadron Collider . . . . .	5
1.4 HL-LHC . . . . .	5
<b>2 Alignment environment</b>	<b>6</b>
2.1 Long Straight Sections . . . . .	7
2.2 Radiation and ALARA . . . . .	9
2.3 Geodetic Metrology group . . . . .	11
2.4 Alignment systems . . . . .	12
2.5 Sensor overview . . . . .	14
<b>3 Sensor support</b>	<b>18</b>
3.1 Design . . . . .	20
3.2 Material . . . . .	22
<b>4 Requirements</b>	<b>23</b>
4.1 Adjustment range . . . . .	24
4.2 Ergonomics . . . . .	25
4.3 Plastic stability . . . . .	26
4.4 Elastic deformation resistance . . . . .	26
<b>5 Tests and results</b>	<b>26</b>
5.1 Adjustment range . . . . .	27
5.1.1 Vertical Shift . . . . .	27
5.1.2 Rotations . . . . .	30
5.2 Ergonomics . . . . .	33
5.3 Plastic stability . . . . .	36
5.4 Elastic deformation resistance . . . . .	38
<b>6 Conclusion</b>	<b>42</b>
<b>7 Appendix</b>	

## Summary

In the context of the High Luminosity Large Hadron Collider (HL-LHC) project at CERN, studies presented in this document describe the validation process of the sensor support prototype that will be implemented in the Full Remote Alignment System (FRAS).

The validation process is based on a series of tests that aim to verify if the sensor support meets the requirements according to the functional specifications, and is therefore suitable to be installed in the accelerators tunnel, where the upgrades for HL-LHC will take place.

The test series provided satisfying results in all the analyzed fields, ranging from technical and mechanical aspects to the design of the components, but also offered the base for several design optimizations that have been developed to improve the prototype.

The sensor support prototype has been validated and will be produced with the proposed modifications in a pre-series production for two test installations. The final series will be implemented together with all other components of the FRAS between 2025 and 2027 on the accelerator components of the HL-LHC tunnel.

# Introduction

Prototype testing and design optimization are key processes in the validation of a component, as they provide the link between the initial prototype and the final product that is ready for series production and that will be installed in the tunnel.

At CERN, the European Organization for Nuclear Research, every component is meticulously validated before being installed, following tailored procedures taking into account the functionality of the product and the specific risks that will be encountered in the installation environment.

The following document describes the evaluation, validation, test and design optimization carried out for the new sensor support that will be implemented in 2025 with the introduction of the Full Remote Alignment System (FRAS) in the context of the HL-LHC project at CERN.

The outcome of these tests has been in first place analyzed at CERN and described in two technical reports [1].

Several tests have been defined and carried out for the validation of the support, evaluating technical aspects like the movement range of the sub-components as well as practical aspects like the ergonomics of the support, concluding with mechanical aspects like the stability of the prototype and its capacity to withstand any external force that might be applied to the support.

This document describes the procedures that have been defined and applied to test each aspect of the prototype, and provides an outcome of the obtained results and the implemented modifications to drive the project to a final version that will be employed in HL-LHC.

After a first introduction to CERN facilities and to the high precision alignment technologies, the document follows in chronological order the requirements, tests and results obtained during the validation process, analyzing all the different aspects that have to be considered in this specific environment and proposing upgrades for the final version of the sensor support.

*“What is the nature of our universe? What is it made of? Scientists from around the world come to CERN to seek answer to such fundamental questions using particle accelerators and pushing the limits of technology.” [2]*

# 1 CERN

## 1.1 Organization

CERN, the European Organization for Nuclear Research, was founded in 1954 with the collaboration of twelve member states and is now the largest particle accelerator centre in the world. Located in Switzerland and France, near Geneva, it hosts some of the world largest and most complex machines, developed to push the boundaries of research and technology. CERN’s international environment is populated by engineers, technicians, physicists and scientists from all over the world, for an overall amount of more than 15000 people working at CERN [3].

The activity of the organization is not only about performing a world-class research in fundamental physics, CERN’s contribution to society regards several fields, such as biomedical technology and aerospace industry. It also has the purpose to train the next generation of scientists and to bring nations together. This information sharing philosophy, where almost everything is public, is well represented by the best-known CERN technology, the world wide web.

This cutting edge technologies developed at CERN are needed as the equipment has to deal with extreme operating conditions, such as vacuum, cryogenic temperatures, radiation and magnetic fields. Because of these conditions new technologies are constantly developed and these innovative solutions are often suitable for other problems elsewhere, thanks to the collaboration with industry for the benefit of everyone.

## 1.2 Particle accelerators

Particle accelerators are one of the main instruments for research in particle physics. They are complex machines, designed with the purpose of accelerating charged particles in order to make them collide onto a target or against other particles circulating in the opposite direction. These particle beams travel close to the speed of light in the form of bunches, where the diameter of the beam can vary. In order to obtain the most possible number of collisions these beams are squeezed in the case of the LHC to a diameter of only 13  $\mu\text{m}$  while reaching the interaction

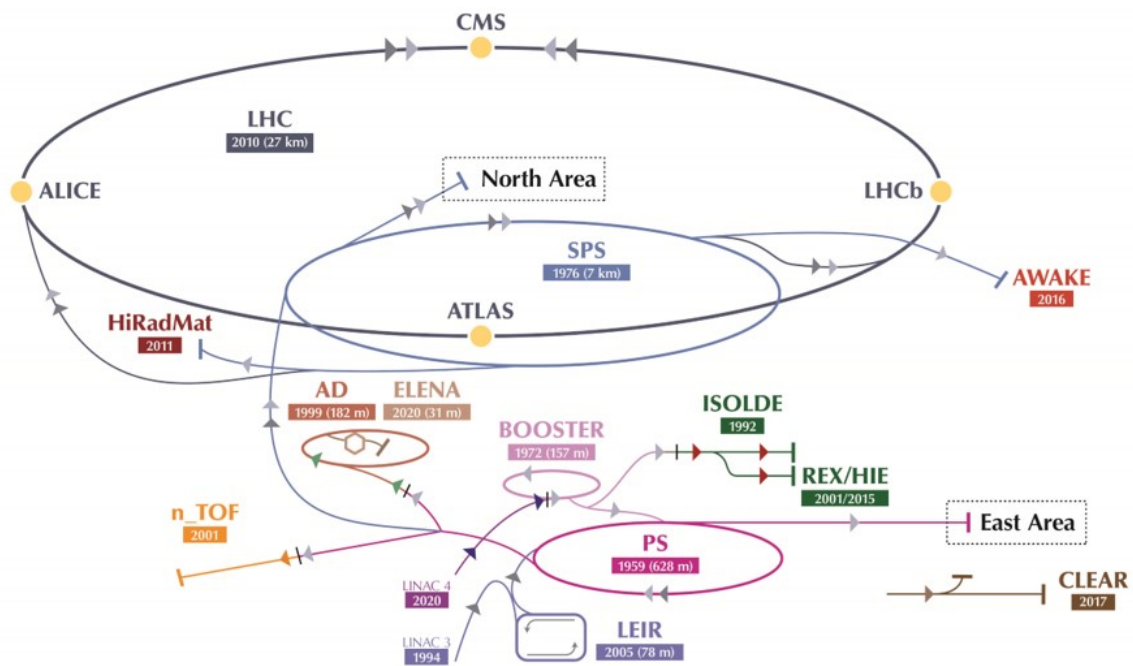


Figure 1: CERN's accelerator complex [5]

point (IP).

With these collisions, new sub-particles are created in the form of exotic particles such as the Higgs boson. These particles are then detected in specific detectors and the data obtained is analyzed by the physicists.

During the more than 60 years activity of CERN several different accelerators have been built [4], beginning with CERN's first accelerator, operating with electrons: the Synchrocyclotron (SC) in 1957 with an energy of 600 MeV.

This first machine was then followed by others that were operating with protons: the Proton Synchrotron (PS) in 1959 and Super Proton Synchrotron (SPS) in 1976, with a continuously increasing level of energy from the 28 GeV of the PS up to the actual 14 TeV of the Large Hadron Collider (LHC) in 2008, as illustrated in figure 1.

Many Nobel-Prize awarded discoveries like the Higgs boson took place at CERN during the years, thanks to the developing of new and more advanced machines and to the collaboration of member states and external partners.



### 1.3 Large Hadron Collider

The LHC is CERN's largest particle accelerator. It was officially inaugurated in September 2008 and still is the largest particle accelerator ever built, with its 27 km of circumference and 14 TeV of collision energy, situated at an average depth of 100 m underground.

Electromagnetic fields are used to guarantee the appropriate shape of the beam, propel the particles and steer them in the correct trajectory. The LHC is composed by a long chain of magnets and other components that allow the circulation of particles and the collision of these particles in the four main experiments.

These electromagnets are placed in an underground tunnel and cooled down to cryogenic temperatures that can reach 1.9 K, operating in superconducting state.

Two beam pipes are situated inside the magnets, to allow the acceleration of a clockwise and an anti-clockwise beam, travelling close to the speed of light. Ultrahigh vacuum is necessary to allow the particles to travel without obstruction by residual gas particles, the vacuum inside the beam pipes can reach  $1 \times 10^{-11}$  mbar.

In the four experiments collisions between particle beams take place and thanks to the detectors physicist can study the composition and properties of these particles. These experiments are: A Toroidal LHC ApparatuS (ATLAS), Compact Muon Solenoid (CMS), A Large Ion Collider Experiment (ALICE) and the LHC beauty experiment (LHCb), distributed along the LHC ring.

### 1.4 HL-LHC

The High Luminosity LHC (HL-LHC) project has been announced in 2013 as the highest priority of the European Strategy for Particle Physics [6].

This project aims to a modification of the LHC facilities, to reach a higher level of luminosity. Mainly the sectors around ATLAS and CMS will be modified towards the HL-LHC transition, and most of the other components along LHC will not be affected by the modifications.

Luminosity in a particle accelerator is proportional to the number of collisions, and is a performance indicator for the machine. More luminosity will allow ATLAS and CMS to obtain more collisions and register more data to study phenomenons which are unreachable with the actual performances of LHC.

With HL-LHC the aim is to increase the luminosity by a factor of ten, but reaching this milestone by improving the actual LHC machine involves new technological challenges on which

most services are currently working.

Following the schedule for the HL-LHC project, all new components should be installed during the Long Shutdown 3 (LS3) and HL-LHC should be operative by the end of 2027 [7].

As part of the mechanical structure to reference alignment sensors with respect to the accelerator components also the investigated sensor support prototype, subject of this thesis, will be implemented in the tunnel.

The sensor support is an integral part of the contribution of the Geodetic Metrology (GM) group to the HL-LHC project.

## 2 Alignment environment

CERN's operational environment is characterized by very different conditions depending on the considered zone of the accelerator. These conditions can be for example cryogenic hazard, vacuum, instantaneous and residual radiation, electrical hazard or strong magnetic fields. They are the reasons why most of the equipment installed in the accelerator complex has to respect a long series of technical requirements.

The sensor support examined in this thesis will be installed in the LHC tunnel, in the proximity of the two experiments ATLAS and CMS. These sections of the tunnel are called Long Straight Sections (LSS), and in there most of the conditions listed above are present.

In order for the complex accelerator infrastructure to work as intended several technological challenges are faced every day, one of which is the alignment problem. More specifically, the problem of aligning the components in the last stages before the collision along the LSS by operating a permanent monitoring system together with a remote alignment system.

The alignment of accelerator components has always been a primary importance problem, because any eventual misalignment can cause perturbations in the particle trajectories, which results in loss of performance. The GM group is responsible for this alignment of all accelerator components.

Since with the HL-LHC project the aim is to increase the performance of the accelerator, improving the alignment of the accelerator components is one of the main ambitions. To face this challenge the GM group is developing the Full Remote Alignment System (FRAS), which is a complex measurement and alignment system of which the sensor support is part of.

## 2.1 Long Straight Sections

Most of the 27 km of the LHC tunnel are in circular shape in order to form the storage ring. The ring is interrupted by eight straight sections of the tunnel, called Long Straight Section (LSS). In these LSS, the beams are conditioned with specific components and the particles are prepared for the collision in one of the four main experiments. One LSS is situated at each side of the main experiments, so a total of four LSS will be modified for HL-LHC in a section of approximately 200 meters, following the scheme in figure 2.

These components vary in shape and function. Some of them will operate in superconducting conditions, involving the use of cryogenic systems to cool down the components to temperatures that can reach 1.9 K, colder than outer space.

The structure of these components is designed to allow the constant refrigeration with the use of liquid helium. They are classified as cold components.

Quadrupoles, identified with Q, are superconducting electromagnets with four poles, working at cryogenic temperatures. The purpose of quadrupoles in the LSS is to focus the particle beam. External dimensions of these components can go up to more than seven meters in length and more than one meter of diameter, with several tons of weight.

The last four magnets before the interaction region are Q1, Q2A, Q2B and Q3; this batch of magnets is called low beta triplet and their aim is to adjust the final focus of the beam before it enters the experiment cavern.

Dipoles, such as D1 and D2, are another example of cold components. Dipoles are also electromagnets like the quadrupoles, characterized by the presence of only two magnetic poles. They are employed along the LSS tunnel with the aim of steering the beam by bending its trajectory, and they are generally longer and heavier than the quadrupoles.

Both for quadrupoles and dipoles the external shielding is the steel-made cryostat, while internally they are composed by several layers of sub-components working at different temperatures.

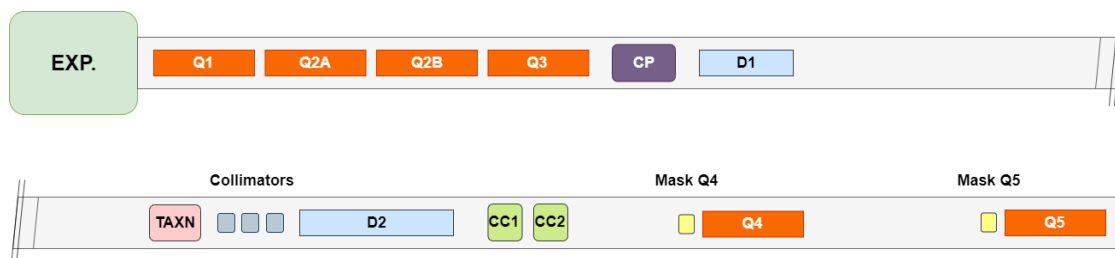


Figure 2: LSS components



Figure 3: Quadrupoles [8]

The assembly of the beampipes with the magnets is the cold mass.

The Crab Cavities (CC1 and CC2) are also cold components, they are more than 3 metres long and have a squared shape.

In HL-LHC, two Crab Cavities will be installed along the LSS, with the purpose of rotating the bunches of particles to a certain angle with which they will then collide. This in the aim to increase the luminosity.

The Corrector Package (CP) is a specific magnet assembly, implemented with the aim of correcting the higher order distortions of the beam.

All other components represented in figure 2 will operate at environmental temperature, which in the LHC tunnel correspond to a controlled temperature between 20 °C and 25 °C. These components are classified as warm components.

Collimators are a member of the family of warm components. Their purpose is to absorb any kind of beam loss and resize the beam. In HL-LHC, a set of three consecutive collimators and several single collimators will be installed. The set of three collimators will result in an overall length of more than four meters.

The Target Absorber Neutral (TAXN) will also be part of the FRAS and provide the transition from two separate to one common beampipe for both beams. The different aims of the presented components are fundamental for the operation of the accelerator and they need to be aligned in a common reference frame to allow for collisions in the experiments.

## 2.2 Radiation and ALARA

As described at the beginning of chapter [2](#), the LSS is characterized by several environmental conditions that affect the technical constraints of the components. Since the sensor support will be installed on the accelerator components, the most relevant hazard to take into account is the radiation resistance.

In this area of the particle accelerator, the radiation is mainly created by particle collisions and the final focus of the beam towards the experiment. These collisions occur both in between particles and between particles and other objects.

When talking about radiation it is important to underline the fact that the radiation to whom an employee can be exposed is not on the same intensity scale as the one to which the components can be exposed in some areas. At CERN the radiation risk is almost null for the employees, thanks to the high safety standards and the strict rules concerning the access to potentially dangerous areas.

The principle followed concerning the exposition of employees at CERN is the As Low As Reasonably Achievable (ALARA) principle, which states that the radiation level to whom a worker can be exposed must be the lowest reasonably achievable.

The amount of radiation to whom an employee can be exposed is reported in CERN safety code [\[9\]](#), corresponding to 1 mSv/yr for non occupationally exposed people and 20 mSv/yr for occupationally exposed employees. The aim is of course to minimize this exposure to the strict minimum.

In table [1](#) some examples of radiation exposure effects given by the world nuclear association are illustrated. As reported the legal annual limit for nuclear employees is 20 mSv per year, but at CERN every year there are no registered cases above 2 mSv/yr, so the reached values are several times smaller than the legal limit, and nowhere close to have any kind of health effect.

The most important safety measure is the limited access to radioactive areas. It is indeed important to distinguish the instantaneous radiation that is only present during beam operation and acts on material from the residual one to which the intervening personnel is exposed to, that is less intense and is decreasing during the shutdown periods.

During the feasibility studies of HL-LHC the accessibility for maintenance reasons was an important topic for the safety aspects. A simulation of how the residual radiation level is going to evolve during the shutdown time in the LSS is given by the FLUKA simulation in figure [4](#). As visible in the graph how the radiation level takes some time before reaching a lower level,

Table 1: Radiation exposure examples [10]

Dose	Cause
2.4 [mSv/yr]	Typical average background radiation experienced by everyone.
5.0 [mSv/yr]	Typical incremental dose for aircrew in middle latitudes.
20 [mSv/yr]	Current limit (averaged) for nuclear industry employees (Europe).
100 [mSv/yr]	Lowest annual level at which increase in cancer risk is evident.
250 [mSv] short term	Allowable short-term dose for workers controlling the Fukushima accident.
1000 [mSv] short term	Threshold for causing temporary radiation sickness, but not death.
10000 [mSv] short term	Fatal within a few weeks.

that is compliant with ALARA requirements.

On the upper part of figure 4 all the components of the LSS are shown from left to right with increasing distance from the IP. The lower part illustrates the radiation level for the different components. Depending on their function, the radiation level will vary for the components.

Concerning the components it is easy to understand how they are exposed to higher doses of

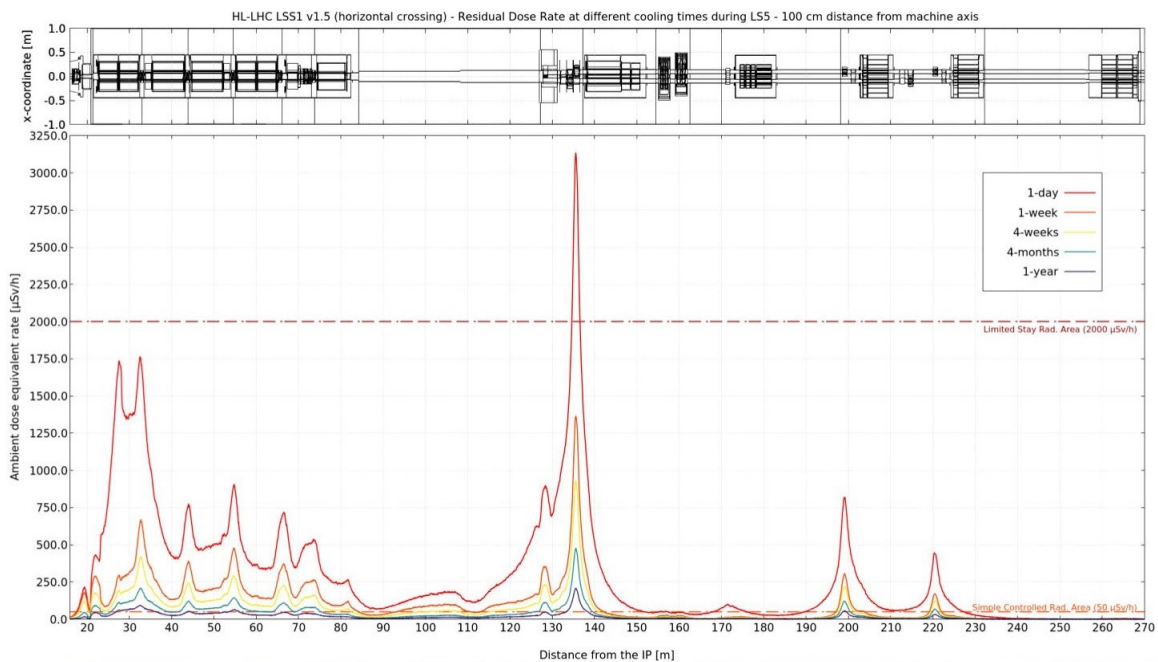


Figure 4: HL-LHC Radiation level P1 along time, FLUKA simulation [11]

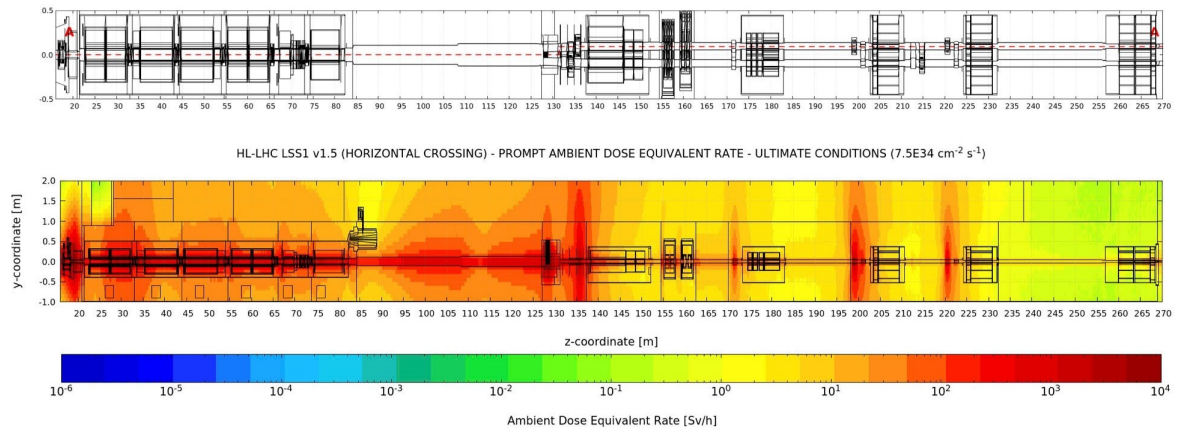


Figure 5: Simulated HL-LHC Radiation level P1 [12]

radiation than the ones described in figure 4, because the radiation to consider is in this case the one reached during operation.

The simulation in figure 5 shows the radiation level during the operation, and can be considered to understand the radiation resistance requirements of the components.

Considering the sensors being situated at a distance of one meter from the components axis it is easy to visualize that the radiation level can easily reach 100 Sv/h in proximity of the collimators, at 135 m from the IP, when the accelerator is running while it is way lower around other components.

These levels of ionizing radiation can cause several problems to the components due to the used material, like cold welding and activation of the material, adding important constrains to the material choice and design of most of the components in the tunnel.

Due to its operation environment the sensor support for HL-LHC is subjected to these constrains, that are determinant also for the tests performed to validate the support.

### 2.3 Geodetic Metrology group

At CERN the group that is responsible for the alignment of all accelerator components is the BE-GM group, where the acronym name stands for: Beams department, Geodetic Metrology group.

The micrometric alignment of the components is divided into two stages: in the first stage the objects are aligned with respect to a reference system and in the second stage of the process they are aligned with respect to each other.

The first alignment is performed directly in the tunnel during the installation of the components

with a laser tracker to a precision of 150  $\mu\text{m}$ .

The second alignment is made for each component with respect to the others in order for the beams to travel through the components fluently. This second alignment, called smoothing, is the one where the highest precision is required and in HL-LHC it will be performed with the FRAS. The instruments adopted are based on different principles and will be able to give online data about the performed alignment and to improve it by moving remotely the components.

For the current LHC machine only components close to the experiment are monitored and adjusted remotely, while the movement of all the other LSS components is performed manually. In the future, with HL-LHC, the new systems for the remote control of components included in the FRAS will allow to adjust remotely the position of all the components without human presence.

## 2.4 Alignment systems

In the LHC environment the axis of the components are defined as follows:

- The radial axis, X, is perpendicular to the tunnel direction. It is the axis that runs from a given point on the component to the hypothetical center of the accelerator.
- The longitudinal axis, Y, is parallel to the direction of the LHC tunnel, it runs along the tunnel and along the component longitudinally.
- The vertical axis, Z, is the one that goes from the considered point on the component vertically to the surface.

The rotation of components in the tunnel around their axes are defined as pitch for a rotation around the X axis, roll for the Y axis and yaw for the Z axis. By modifying the three rotations and the three translations of the components it is possible to reach the desired alignment.

The alignment system that is currently employed in the LHC has been developed by the GM group. It is constituted by several components like motors, sensors, supports and their electronic parts.

The sensor network registers the position of the components using different types of sensors. The position information is then used to calculate the required movement to reach the ideal alignment position and with a series of motors the components are moved and lifted to reach this position.



As the components will be replaced for the HL-LHC upgrade, this old system will be replaced by the FRAS system, to allow an entirely remote alignment for each component in the tunnel, thanks to the sensors that will give constant feedback about the position of the components and the motors that will allow remotely controlled movements.

The sensor support is an important part of the FRAS, as it will host two of the main sensors employed for the position determination.

Considering that, as described in section 2.1, the dimension of the components can reach several meters in length and many tons of weight adjusting their positions is challenging, especially if with the aim to reach micrometric precision.

The components are guaranteed with five degrees of freedom, three rotations and two translations. The movement system for each component is developed to ensure micrometric precision in short range movements, to do so two different systems to move the components have been designed for the FRAS:

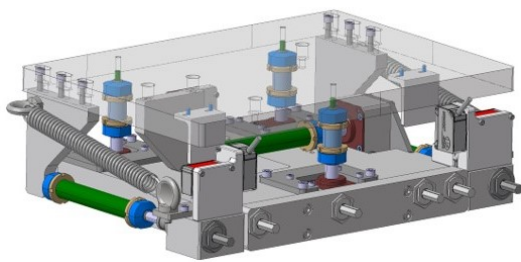


Figure 6: UAP for HL-LHC [13]

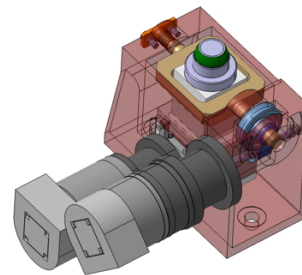


Figure 7: Jacks for HL-LHC [14]

- Universal adjustment platform (UAP). For light components, weighing less than two tons and limited in dimensions, the adopted solution is the UAP, as illustrated in figure 6. The UAP is designed to sustain and align the components with five (optional six) degrees of freedom, thanks to a series of motors that will be activated remotely. In this solution the component is fixed on the top plate of the platform and it is the whole top plate to move, moving the component and adjusting its position.
- Jacks. To sustain heavy components, weighing more than two tons, the adopted solution is based on jacks, for which an example is given in figure 7. The basic configuration is with three jacks for each components, where each of them can be activated singularly, so that each rotation and translation is achievable with a different combination of linear movements.

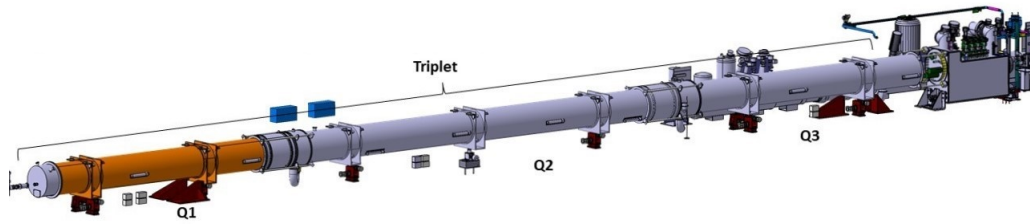


Figure 8: Schematic representation of the LHC triplet in 5R

These linear movements are performed with different motors and screws to move horizontally the components.

Figure 8 illustrates a schematic representation of how the triplet in point 5R looks like now in LHC, with the red jacks under the magnets.

## 2.5 Sensor overview

With the HL-LHC project all components in the concerned sections will be removed and the new ones will be installed from scratch, together with them also the sensor network to track the position of the components will be removed and replaced with all the new systems.

The sensor support will be fundamental for the operation of this network, allowing the installation of the majority of these sensors. Taking a magnet as example, a simplified overview of how the sensors will be positioned is given in figure 9.

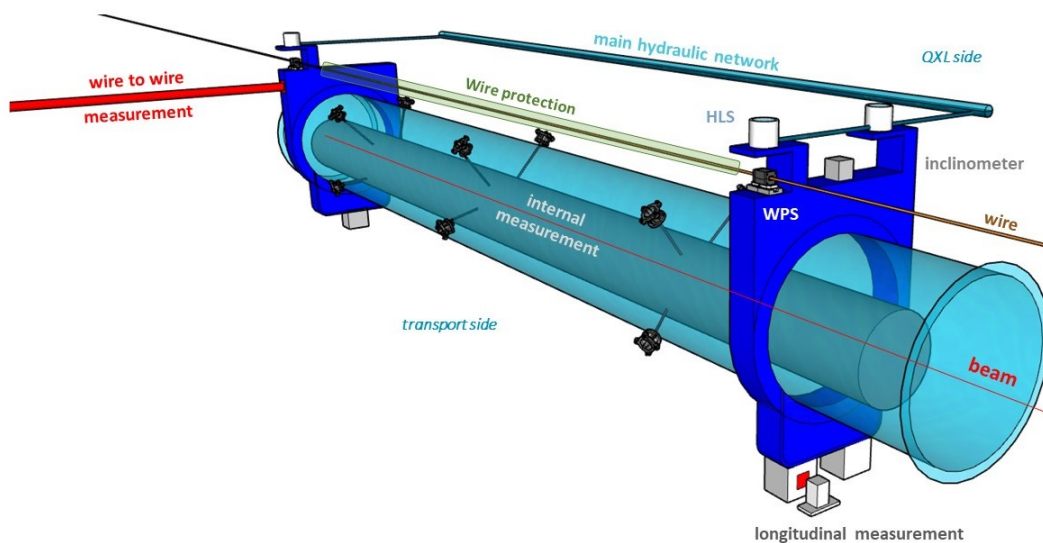


Figure 9: Simplified sensors overview [15]

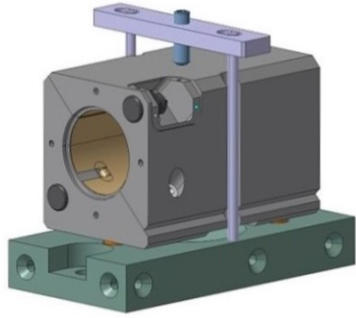


Figure 10: WPS HL-LHC [16]

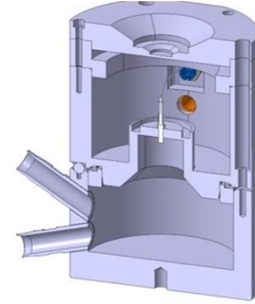


Figure 11: HLS HL-LHC [17]

The types of sensor and their configuration will essentially remain the same for HL-LHC, with the Wire Positioning Sensor (WPS) and the Hydrostatic Levelling Sensor (HLS) as main protagonist and several other sensors to complete the position control of the components:

- WPS. The WPS is constituted by four electrodes that measure the distance from a wire. It is used to measure the displacement of the components to which it is attached with respect to a stretched wire, serving as straightness reference.

In figure 10 the sensor itself is grey, while in green the isostatic 3-ball interface is represented. This interface serves as link between the sensor and the support, to which it is fixed with two screws. Having the isostatic interface as contact points with the sensor it allows a position repeatability of the sensor to 1  $\mu\text{m}$ . The cross-section of the sensor is shaped to allow both horizontal and vertical measurements, in a working range of 10 mm for each axis with a resolution of better than 1  $\mu\text{m}$  and an absolute calibration of better than 5  $\mu\text{m}$ .

By equipping a component with at least two of these sensors like illustrated in figure 12 it is possible to know the position and calculate the angle of each component.

To provide better redundancy a second WPS line will be added on the other side of the component for the most critical section between Q1 and D1. With four sensors it will be possible to calculate the rotation around Y.



Figure 12: WPS sensors in the LSS

- HLS. The hydraulic levelling sensor will be changed from capacitive measurement technology to multi-target frequency scanning interferometry for the HL-LHC. The new sensor is represented in figure 11. The HLS consists of a measurement vessel filled with water and an optical fibre tip that measures the distance to the water surface.

This sensor is used along the LSS tunnel to monitor the vertical displacement of the considered component with respect to the local gravity and also to calculate the roll and the pitch angle of the component thanks to the principle of equipotential surface.

All the HLS sensors along the tunnel are connected through a water network, as illustrated in figure 13 and with an air link to exclude pressure variation in between the measurement vessels as this would influence the equipotential surface and thus destroy the measurement reference.

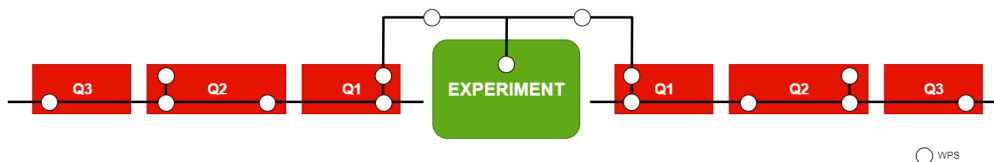


Figure 13: HLS sensors in the LSS

- Others. Several different systems are employed to determine the position of the components, like the longitudinal monitoring system (LON) which will be placed under each component to measure the position along Y with respect to a fixed point.

Other sensors like the internal monitoring sensor (INT) are employed in components such as Q1, Q2A, Q2B, Q3 and the crab cavities to monitor the position of the cold mass inside the cryostat.

To link the position of the components from one side of the interaction region to the other side, the Invar Rod System (IRS) is currently in use in the LHC. This system is composed by a rigid invar bar that links the triplet to a parallel tunnel, which is then connected to the experiment's cavern.

In HL-LHC the rigid link between the two galleries that characterizes the IRS will be replaced with a frequency scanning interferometry laser system, introducing the Wire to Wire system (W2W).

In addition, several components will be equipped with an inclinometer (INC), that measures the inclination of the component around the Y axis.

It is evident how all these sensors provide measurements that can be redundant, for example if we consider the roll of the components it can be measured both with the HLS and the inclinometer, while the pitch can be measured with the HLS and the WPS. This redundancy is important to guarantee that it is always possible to measure each parameter of each component, even in case of failure of some of the sensors. With the actual configuration of the LHC the length of the monitored components is roughly 40 m, but with the HL-LHC it will reach approximately 200 m on each side of the experiment.

One single WPS wire runs along this 200 m section, connecting all the components in the measurement chain. Despite the wire will be stretched from one side by a given load it will be characterized by a sag that shall not exceed 100 mm [19].

Along its 27 km of length the LHC tunnel is characterized by a certain slope, which in some sectors can rise up to  $1.5^\circ$ . More in detail also the LSS sectors in point 1 and point 5 are characterized by this slope, which in the 200 m of length of the tunnel results in a drop of roughly two metres.

The WPS wire has to follow the slope of the tunnel, together with all the WPS sensors, while the HLS network needs to be levelled with respect to the local gravity.

The HLS network has then to cover several steps along the LSS tunnel to cope with the slope, these steps require a double HLS, where the upper sensor is levelled with one layer of the network and the lower one with another layer, as illustrated in the scheme of figure 14.

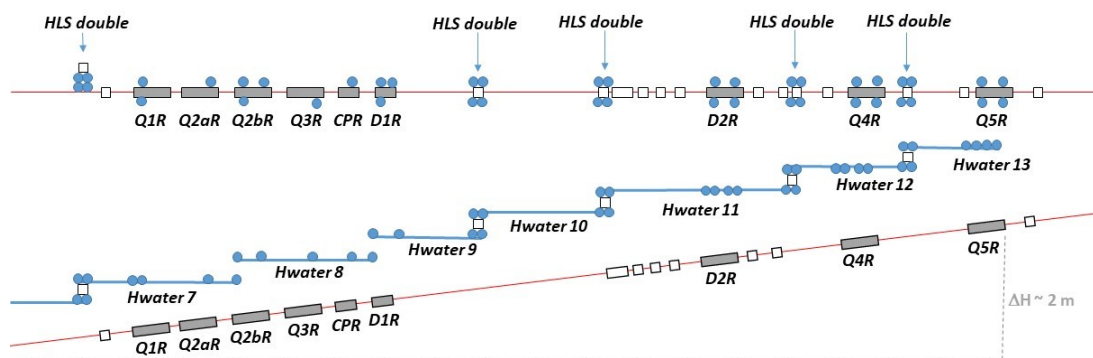


Figure 14: HLS steps in tunnel

### 3 Sensor support

HLS and WPS are the most numerous sensors in the FRAS network, with 43 HLS and more than 50 WPS sensors for each side of the experiment.

Both sensors need a rigid interface to be linked to the component, the interface has to adapt to the different shapes that characterize each component, reducing the cost of several different projects and promoting the interchangeability of the FRAS equipment. Moreover, from the LHC experience, the GM group has had the experience to see all the advantages of a versatile support that can be easily separated from the component.

The interface that will be employed to fix the WPS and HLS sensors to the concerned components is the sensor support for HL-LHC, illustrated in figure [15](#). The aim of this support is then to provide an interface that can be employed for the majority of the LSS components, independently from where in the tunnel the support will be installed.

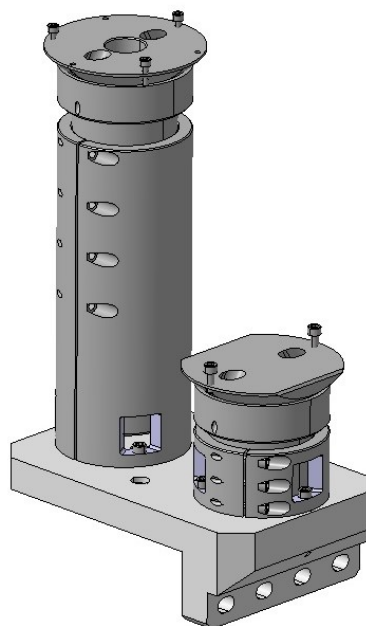


Figure 15: Sensor support 3D model

The standard sensor support for HL-LHC will be implemented for the FRAS on the components: Q1, Q2A, Q2B, Q3, CP, D1, D2, TAXN, Q4 and Q5.

The sensor support debated in this project is a prototype of the final component, with the aim to validate the design and implement all the modifications before the pre-series production. As reported in section [1.4](#), the FRAS for HL-LHC have to be ready by the end of LS3 to be operative in 2027, whereas the supports have to be installed at an earlier stage, starting in 2025.

Despite being a static component of the FRAS, the sensors support has a long list of requirements to fulfil, as defined in the functional specification [18].

To guarantee the needed stability of the measurement each sensor in the tunnel has to be rigidly fixed on the considered component through the sensor support. All space available in the tunnel is precisely distributed in between the groups, to allow the installation of each instrument in the limited space that the tunnel offers. The support has to guarantee the position of the sensors inside the dedicated space during all its lifetime, without interfering with the transport volume. The stability requirements are to a couple of micrometres.

In most of the cases, the HLS sensor and the WPS sensor will be installed one next to the other on the sensor support bracket interface on the component. Each of them is independent from the other. Indeed, the HLS must be positioned at the corresponding height of the hydraulic network, because it has to follow the steps of the network, as described in section 2.5. It also needs to be levelled to local gravity in order to have a perpendicular measurement to the water surface inside the measurement vessel.

The WPS instead needs to follow the position of the wire and the sag of the wire, following the tunnel slope as described in section 2.5, and the sensor support has to guarantee the position of the sensor with a certain offset from the beam axis.

The sensor support is designed to be installed in both sides of the components and to be accessible during maintenance operations. An example of component equipped with the sensor support is given in figure 16, where two sensor supports are installed on the right side of Q5.

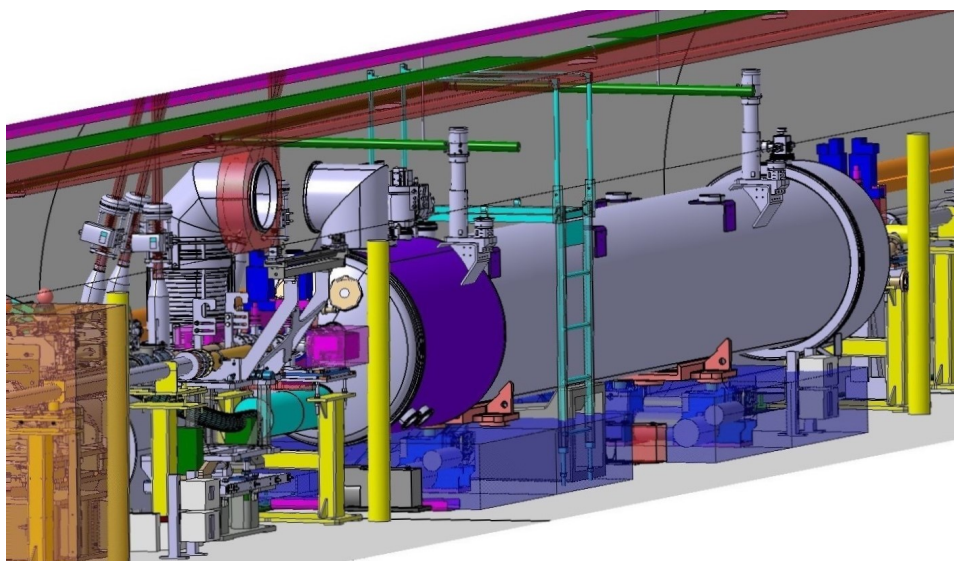


Figure 16: Sensor support on Q5 3D view

### 3.1 Design

The design of the sensor support aims to fulfil the series of requirements as defined in the functional specification whilst at the same time providing a cost effective solution for the approximately 200 items production.

As introduced this will be necessary to adjust the position of the two sensors independently. To do so the sensor support is provided with two separated columns, one hosting the HLS sensor and the other hosting the WPS.

The WPS column is shorter than the HLS one, since the height adjustment range needed by the WPS is lower as it follows the tunnel slope and not the steps of the hydraulic network.

As introduced at the beginning of this chapter, the sensor support will be installed on almost all the components in the tunnel, but since each component has its own shape an additional interface where to fix the support is needed.



Figure 17: Sensor support in the TAP

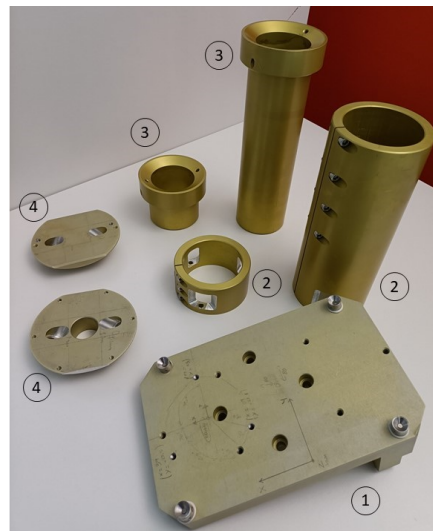


Figure 18: Sub-components

For cylindrical shaped components, like all superconducting magnets, the complementary support is the Sensor Support Bracket (SSB), represented in figure 17 as item ②.

The steel made SSB is rigidly welded to the cryostat and offers two flat and perpendicular surfaces where to fit the sensor support.

The sensor support, marked as ① in figure 17, is made of seven sub-components, which are illustrated in figure 18:

- Sensor support base: it is the squared plate on the bottom side of figure 18, labelled as ①. It is designed to be fixed on the horizontal plane of the SSB with four screws vertically



and two screws from the radial side.

The support base provides a stable sole where to install the columns and all the other sub-components of the sensor support.

- Support tubes (bottom part): The support tubes, marked as ②, are the external part of the columns, they are designed to hold the top tubes and guide them during the vertical adjustment.

They are fixed on the support base with three screws each and they have screws in the sides to clamp the internal tubes at a given height, once the desired position of the sensor is reached.

- Support tubes (top part): Positioned on the top part of figure 18 and labelled as ③, these are the internal tubes which slide inside the other support tubes. In figure 20 a cross section of the WPS support tube is illustrated. Their position is set by using the horizontal screws in the support tubes. The top tubes are designed to host the tilt lenses, on which the sensors are fixed.

- Tilt lenses: the aim of these components is to host the sensor and adjust its roll, pitch and yaw; they are marked as ④ in figure 18.

As illustrated in the plans of figure 19, the geometry of the tilt lenses is divided into a flat surface on the top, where the sensor is fixed with two screws, and a semi-spherical surface on the bottom that fits on the upper tubes and allows the lens to rotate.

The two tilt lenses of WPS and HLS have different fixation possibilities, in order to allow the HLS measurement vessel and the WPS 3-ball interface plate to be installed on them.

The HLS tilt lens has a hole perpendicular to the flat surface that allows a spherical level to be inserted, this process is necessary to level the HLS tilt lens.

The sensor support considered for the tests is only a first prototype, indeed the purpose of the tests is not only to validate the component and its characteristics, but also to propose eventual improvements, driving the project towards a final design which will then be adopted for all the sensors supports in the FRAS system.

As an example the number of screws employed in the support tubes to fix the position of the top tubes is a consideration that had to be discussed during the test of the support. In the tested prototype the number of screws where four for the HLS columns and three for the WPS column, but during the validation also a test with a reduced number of screws has been performed.

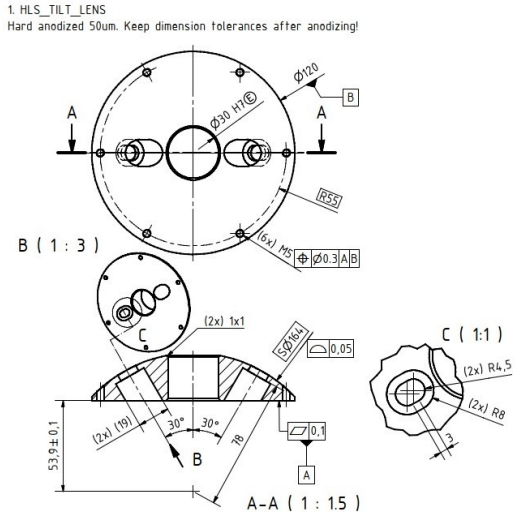


Figure 19: Tilt lenses plans

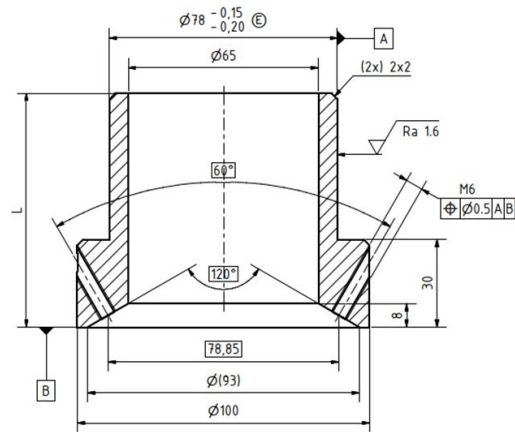


Figure 20: Cross section support tube

### 3.2 Material

When choosing the material for a component operating in the particle accelerator, it is important to follow the CERN guidelines. There are several parameters to consider when choosing the material for a component operating in the tunnel, where normal specifications like rigidity, manufacturability, reliability and cost are not enough.

The material choice for the sensor support follows the general safety instructions stated by CERN, which regulates the use of every kind of material depending on fire risk and other hazards [20].

As it will be installed along all the LSS tunnel the particular conditions it will have to deal with are described in section 2.2. The main challenge the sensor support will have to deal with during the 15 years of operation is the radiation level of the area where it operates, and for the material choice the radiation is of course a major factor.

For the sensor support the main problems related to the radiation exposure over the years are the possible formation of rust, the creation of cold welding due to radiation in the movable parts of the component and the activation of the material.

Cold welding could be a problem in the sensor support for the internal surface of the columns, since the position of the sensor will remain fixed for a long time and in case of future adjustment it could be then problematic to move the sliding tubes.

To avoid the problem of cold welding and the possible formation of oxides on the surface of the sub-components the sensor support prototype are made of aluminium and have been anodized.

The activation of the materials is a well known problem at CERN in the environments that are exposed to beams, indeed the residual radiation in the LSS tunnel described in figure 4 is partially given by how the material gets activated by the radiation.

To limit the activation of the components the materials must be chosen wisely, by optimizing the chemical composition and in some cases excluding entire groups of materials.

To avoid complex and time consuming analysis for every single component to be implemented in the tunnel a specific software called ActiWiz has been developed at CERN [21]. With this software it is possible to estimate the activation of the material considering the position with respect to the beam and its chemical composition.

Steel for instance has strict limitations for certain alloy elements, for example the quantity of cobalt. Specifically the problem is the formation of radioactive isotopes like  $^{60}\text{Co}$  and in any kind of steel  $^{55}\text{Fe}$ , which decay emitting ionizing radiation. As a general rule, the use of aluminium is usually advisable as substitution of common steel for components operating in the tunnel whenever possible. The sensor support is no exception to this general rule, being made of EN-AW 6082, aluminium of series 6000, containing then magnesium and silicon.

## 4 Requirements

Every component has to be tested before the installation in the LHC environment, to assure that it meets the requirements and minimize the need of further intervention during the operational time of the accelerator.

Even ordinary maintenance processes can be problematic in the LHC, because each intervention has to be performed respecting the operative schedule of the accelerator and it is not always possible to have access because of the presence of other groups or ALARA restrictions.

As for the other components also the sensor support will have to ensure its operation during all the years of HL-LHC activity while guaranteeing the technical requirements:

1. Adjustment range, to provide a sufficient position adjustment range to the sensors.
2. Ergonomics, to ensure the needed precision of the adjustment in a time coherent with the needs
3. Plastic stability, to preclude permanent modification of the position of the sensors that may occur due to an applied force.

4. Elastic deformation resistance, to prevent excessive movements of the sensors when a force is applied.

The technical requirements of the sensor support are a consequence of the conditions where it will be installed in HL-LHC. Following the technical and functional specifications, these requirements were the objects of the validation and are reflected on the four main test categories performed on the sensor support prototype.

## 4.1 Adjustment range

One of the main requirements for the sensor support is to provide a sufficient position adjustment range for the sensors.

As described in section 3.1 the sensor support is composed by one column for each of the two sensors to adjust the height and two tilt lenses on top of each column to adjust the rotations around each axis.

The adjustment range is important to guarantee the position of the sensors with respect to the beamline, which has to satisfy a precise offset, and with respect to the HLS water network and WPS wire reference.

The adjustment along Z is fundamental for the HLS sensor to be always on the same height of the other sensors in the same step of the hydraulic network, as illustrated in figure 14.

The vertical adjustment range also allows the WPS sensor to cope with the wire sag, its column should indeed have an adjustment range along Z of at least 20 mm, because as foreseen in section 2.5 the overall sag of the wire in the 200 m long tunnel will be approximately 100 mm, so a minimum of five sub-types of the WPS sensor support column are needed to cover the whole length of the tunnel.

Consequently for the HL-LHC final application the WPS support will be designed with different lengths depending on where along the LSS tunnel it will be installed, so that the sensor can follow the wire position along Z.

The inclination range of the tilt lenses was also an important parameter to be tested, because the tunnel in Point 1 and Point 5 is characterized by a slope of up to  $1.5^\circ$  of inclination.

Since the HLS sensor needs to be levelled to allow perpendicular measurement to the water surface and the WPS sensor has to follow the tunnel slope the inclination range that the tilt lenses should provide is at least  $\pm 1.5^\circ$  around X and Y.

For the rotation around Z of the HLS tilt lenses the range can be limited since due to the mechanical limitation it can only provide minor movements, with a maximum of  $\pm 0.3^\circ$ . For the WPS tilt lenses this rotation value can then additionally be compensated by the presence of the 3-ball interface, so that the sensor can always be oriented along the reference wire, parallel to the y axis.

## 4.2 Ergonomics

As reported in section [2.2](#), limitations due to radioactivity are the main constraints for the future FRAS and this has of course consequences on the specifications of the sensor support.

At CERN every operation has to be performed following the ALARA principle, meaning that the radiation exposure of the employees must be as low as possible in relation with the situation. Considering for example the values given by the simulation in figure [4](#) in the area close to the low beta quadrupoles the level is close to 0.10 mSv/h after four months of stop, such amount of radiation translates in only ten hours of work close to the magnet to reach the level of the highest accumulated exposure at CERN, corresponding to 1/20 of the year limit.

This simple calculation explains why the sensor support as well as all the other components installed in the tunnel need to be ergonomic. The approximately 200 sensor supports will be installed and maintained on site and therefore the personnel will be exposed to radiation. The sensor support has to be ergonomic and fast to be assembled, to minimize the exposure of the personnel to this risk.

The required adjustment precision has to be better than  $0.3^\circ$  for the rotations of the tilt lenses and 0.3 mm for the translation along Z of the columns. This precision is the one to be reached during the installation, in the shortest time possible following the ALARA principle.

In order to reduce the assembly time as much as possible, the ergonomics of the sensor support must be optimized at its best, including for example an analysis of the minimum number of screws or the best optimization of the shape to facilitate the assembling process of each sub-component.

### **4.3 Plastic stability**

In normal operative conditions the sensor support must not be subjected to external forces, nevertheless during its operation accidental impacts might apply temporary forces to which it has to withstand in order to keep its parameters.

The BE-GM group has experienced along the years several cases of deterioration of the supports, whilst all the warning labels and the protections applied to the equipment.

With this experience, these unexpected forces must be considered when designing the supports, to minimize the risk of damage and unnecessary interventions in HL-LHC.

During the LHC operation, one of the most common problems was the use of the supports as handle to access equipment on or behind the components on which they were fixed; resulting in potential plastic deformation of the sensor support columns, which would remain permanently when the force is removed.

Any eventual plastic deformation brings unknown errors in the position determination of the components. An on site intervention would be needed for repair and alignment measurements. Therefore the sensor support must not deform permanently if a force is applied.

The amount of screws used to fix the top tubes in the final position and the orientation of the screw slots with respect to the tunnel are crucial parameters to consider for the rigidity.

### **4.4 Elastic deformation resistance**

The elastic deformation resistance of the support is also an important parameter, because since the support will host sensors with micrometric precision every movement of the support due to external factors will be registered by the sensors and might transmit data that does not correspond to the actual position of the component to be aligned.

Some sub-components like the HLS column are particularly exposed to deformation because of its size, reason why the sensor support has to be tested to assure that in case of misuse no permanent damage will occur.

## **5 Tests and results**

The chronology of the validation process for the sensor support followed the order of the requirements described in chapter [4](#). These prototype tests were not standardized to control a series production, but specifically tailored to the sensor support in order to investigate that it

complies with the functional specification.

These tests were validated in laboratory conditions before being carried out in real tunnel conditions. They were indeed performed in the laboratory to assure that the results were reliable in an environment with constant temperature and humidity, and then the same tests were carried out in a real test environment simulating tunnel conditions.

In this second facility the support was installed on the Twice Aperture Prototype (TAP), which is a disused magnet, where the only outer cryostat of a dipole is made available to test different kinds of equipment. All the data reported in this document comes from the tests performed on the TAP, because they offer the most reliable data since the SSB where the support was fixed was welded on the magnets cryostat, as it will be in the final application of the support.

A laser tracker has been used during the tests to determine the position of the components and their movements with micrometric precision. The laser tracker carried out angle a distance measurements to a spherical target prism and therefore allows a three-dimensional analysis of the movements. The reference positions of these targets are represented by the fiducials, which are conic supports.

A bubble level has been employed to adjust the rotations of the tilt lenses to the desired position and an inclinometer has then been used to verify the reached inclination precision.

## **5.1 Adjustment range**

The first test performed on the sensor support was the adjustment range check to verify both criteria: the reachable height with the top tubes of HLS and WPS as well as the rotation range of the tilt lenses. The test was divided into two parts, one dedicated to the vertical shift and one to the rotations.

### **5.1.1 Vertical Shift**

To quantify the vertical shift range of the sensor support that still provides a stable position, the height difference between the bottom position and the top reachable stable position of the tubes was measured, as illustrated in figures [21](#) and [22](#).

To precisely determine the height difference along the Z axis, the employed tool was the laser tracker using a 1.5 inch target installed in a fiducial on the top surface of the tilt lens.

To measure the range the initial position was determined and assigned as origin of the axis, then the column was lifted to the maximum stable height and the measurement was taken in

Table 2: HLS lifting range

Position	Tz [mm]	Tav [mm]
1	188.500	187.540
2	189.170	
3	184.941	

this position without moving the target.

For statistical reasons the process was repeated three times and subtracting the two values the vertical range reported in table 2 was obtained. The result is more than satisfying, with more than 180 mm of range.

Operating with the HLS column at its maximum extension of 190 mm during the adjustment process whilst not having the screws entirely fixed can be dangerous. The risk of the unintended dropping of the column in case of not tight enough fixation is a potential dangerous situation dangerous for both the operators and the components, especially if during maintenance processes, where both the hydraulic network and the WPS wire are connected to the sensors.

To solve this safety issue, a solution was developed by proposing a simple, 3D-printed ring that holds the HLS top tube in position while fixing the screws. This ring was designed in the first version with a simple one screw fixation system, as illustrated in figure 23. For the real



Figure 21: Lifted HLS



Figure 22: Lifted WPS



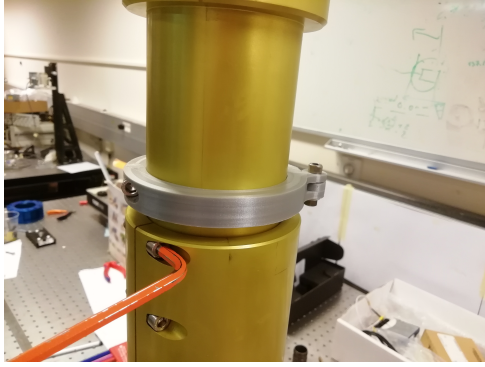


Figure 23: 3D printed ring prototype

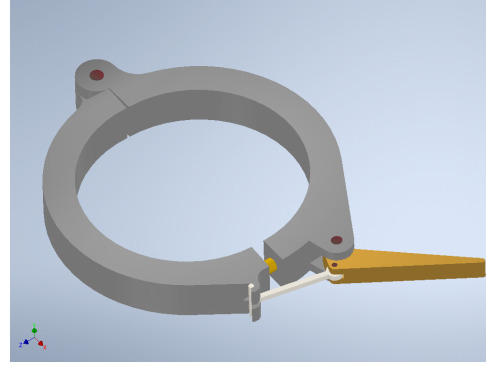


Figure 24: Ring model with clamp

installation of the supports during LS3 also a more ergonomic version with a clamping system, illustrated in figure [24](#), has been designed and will be tested in the future.

For WPS also the translation along the radial axis has been measured, because with these wire based sensors the radial adjustment range is important to assure that the wire is centered in between the electrodes.

The translation range along X is given by the three ball interface, more in specific by the fixation slots of this interface.

The position of the 3 balls interface has been measured with the laser tracker similarly to how it was for the lifting range. The obtained values are reported in table [3](#).

Table 3: WPS lifting range

Position	Tz [mm]	Tz av [mm]	Tx [mm]	Tx av [mm]
1	29.47	30.31	32.75	32.83
2	30.78		32.87	
3	30.69		32.88	

During the vertical shift range check some manufacturing related issues concerning the applied tolerances were encountered when lifting the WPS tube.

Therefore it was not easy to move the WPS top tube because of too tight manufacturing constraints between the internal and external tube blocking the vertical movement.

Since the issue was only concerning the WPS tube and not the HLS one the conclusions were that the problem was in the tolerance of the WPS support tube, that was not properly realized by the manufacturers in this prototype. As the tubes are anodized it cannot be distinguished if the problem was due to the initial dimensions of the piece or due to the anodization.

In a medium or large scale production of mechanical components it can happen that some tolerances are not perfect, but in this case to move the WPS top tube it was necessary to use a screwdriver and force the closure of the support tube, increasing considerably the needed time for the position adjustment.

To avoid the necessity of changing part of the columns in case of manufacturing error, for the final version of the sensor support the manufacturing drawings will be updated and require the tolerances to be met after the anodization process. Like this, the manufacturer has to provide the functionality of the top tube moving freely inside the support tube without interference.

### 5.1.2 Rotations

The procedure to measure the rotation range of the tilt lenses has been the same for the first measurement campaign in the laboratory and the second one in the TAP.

The considered tilt lens was rotated until one of the two extremities of the rotation range was reached and then fixed in this position. The angle with respect to local gravity was then measured with the inclinometer and the procedure was repeated for the other extremity and for statistical reasons with three iterations.

By adding the two inclination values in the two directions the adjustment range was obtained. A summary of the adjustment range for the rotations is illustrated in table 4. These values are the average of three iterations, calculated from the detailed measurements provided in tables from 16 to 19, which can be found in the appendix of this document.

Table 4: Rotation range overview

Unit	[mrad]	
Rotation	Rx	Ry
HLS	96.708	50.068
WPS	101.431	50.122

As reported in section 4.1, the minimum desired adjustment range is  $\pm 1.5^\circ$  ( $\pm 26$  mrad) for Rx, and it was almost doubled. For Ry and Rz there was no specific requirement but the values obtained are largely sufficient.

For the WPS sensor also the rotation range around Z is an important parameter, because the orientation of the sensor has to be parallel to the wire.

Table 5: Rz rotations overview WPS

Unit	[mrad]	
Rotation	Rz 3 balls interface	Rz tilt lenses
WPS	490.266	91.524

The rotation range around Z is determined by the tilt lenses and the three ball interface that will later host the sensor. These have been tested separately. The obtained data concerning the rotation range around Z is reported in table 5 for the two cases.

As for the other data in this document the reported values are obtain as average of three iterations, the complete tables are reported in tables 20 and 21 in the appendix.

For the 3 balls interface the rotation was measured indirectly using two points to create a straight line on the side of the 3 balls interface, and verifying the inclination of this line with respect to the reference, as illustrated in figures 25 and 26.

During the rotation range test of the tilt lenses the first issue encountered was the impossibility of having a smooth movement of the tilt lenses when sliding on the support. To have a more fluid movement of the tilt lenses and use their full adjustment range it was necessary to apply grease on the contact surface. The chosen grease was the radiation resistant version Petamo GHY 133N.

With the use of grease during the tests the smoothness of the movement improved drastically,



Figure 25: 3 balls interface Z rotation



Figure 26: 3 balls interface Z rotation



Figure 27: Bigger washer



Figure 28: Smaller washer

so this lube will be employed also for the final application of the sensor support.

Concerning the rotation of the tilt lenses an issue was encountered with the washers. They were supposed to fit in the upper holes to fix the position of the lenses, but as illustrated in figures 27 and 28 the outer diameter of the washers was not specified. Several tests were needed to find the correct washer as some of them were too little for the holes, some of them too big.

To verify the effective influence of the presence of the washers in the fixation holes and spot an eventual limitation of the range caused by the interference with the bigger washers, the rotation range was tested twice with the use of the bigger washers and without any washer.

As reported in table 6 the difference in terms of movement range between the two options was negligible and the required range was comfortably reached in both the cases.

Table 6: washers influence [mrad]

[mrad]	Required		w/o washers		with washers	
	Rx	Ry	Rx	Ry	Rx	Ry
HLS	52.4	34.9	108.2	49.1	96.7	50.1
WPS	52.4	34.9	111.9	53.2	101.4	50.1

Nevertheless using the bigger washer was not an option, because even if it was not hindering the movement of the lenses its external diameter is the same as the width of the screw socket, so the washer risked to be stuck.

To try and solve this issue several different washers have been tested, both standardized and non standardized ones, but none of them was fitting.

The solution for this problem will be to use the bigger standardized washer and modify the

sockets in the upper part of the tilt lenses, by widening them of 1 mm, to fit the washer in any position of the lens. All the modifications concerning the tilt lenses have been added to the plans, to be implemented in the final version of the support.

## 5.2 Ergonomics

The second requirement to be tested was the ergonomics of the sensor support. The test consisted in a validation of the required time to adjust the sensors to the final position and with the desired precision.

To operate it in a realistic way, the support was fixed on a sensor support bracket which was welded on the cryostat of the TAP prototype cryostat; the height of the support was approximately 1.80 m above the floor and the sensors were lifted up to halfway the adjustment range.

The considered process was a complete position adjustment, involving:

- Lifting along the Z axis by moving upwards the support tubes and fixing them at a given position. The position was fixed to a predefined target value along the extension range, that was previously assigned as zero of the axis.
- Adjusting the rotations of the tilt lenses around Rx and Ry to level the position, with the use of a level and allen keys to fix the two screws.
- For the WPS also the translation along X and the rotation around Z was adjusted, by moving the 3 ball interface.

The adjustment process was managed as similar as possible compared to the real assembly of the support during the HL-LHC installation. To gather information about the installation position, laser tracker measurements provided the real-time position and were used for feedback in the adjustment process by displaying these values on a laptop.

The adjustment process was performed by two operators to include in the measurements the influence of various operators. During the position adjustment there was a minimum and an optimal precision to be reached, reported in table 7.

The bubble level itself has a precision of  $\pm 1.5$  mrad for the Rx and Ry rotations and the laser tracker 11  $\mu\text{m}$  from the considered distance.

The main target of the ergonomics test was to obtain the required time for this adjustment, referring to the precision in table 7, and to identify any possible mechanical modification for a

Table 7: Precision requirements

	Minimum	Optimal
Translation (Z) [mm]	1	0.3
Rotations [mrad]	17	0.6
Rotations [deg]	1	0.3

more ergonomic use, that has be implemented in the final version of the support.

All the data obtained from the test is reported in tables 8 and 9. The full version of these two tables are reported in the appendix, showing in tables 22 and 23 the required time for each intermediate step of the positioning adjustment process of the sensor.

Table 8: WPS ergonomics

Iteration	Operator	total time [ss]
1	B	07:45
2	A	08:05
3	A	06:30
4	B	09:05
5	B	05:54

Table 9: HLS ergonomics

Iteration	Operator	total time [ss]
1	A	02:45
2	A	02:00
3	B	03:10
4	B	02:55
5	B	05:14

As pointed out in the tables, the required precision was easily reached in an acceptable time in all the iterations.

One of the main purpose of the ergonomics test was to get in confidence with the assembling of the sensor support and find where little improvement of the initial design could be implemented, to simplify and validate the assembling process.

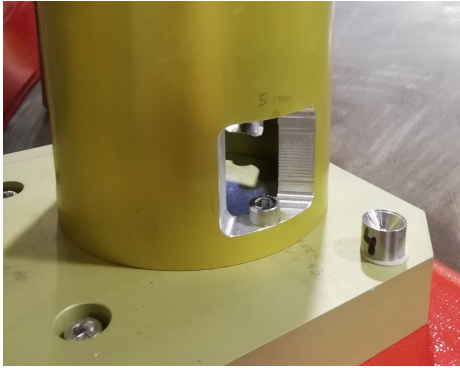


Figure 29: Widened socket, HLS

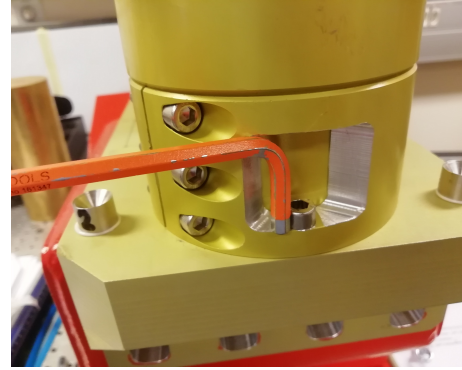


Figure 30: Socket issue, WPS

As expected several little modifications of the original design have been identified and will be implemented in the final version of the sensor support for HL-LHC.

One of the first modifications of the plans was concerning the dimension of the sockets that host the screws to fix the support tubes to the support plate. These sockets, as shown in figure [29](#), have been widened both in the HLS and WPS column, increasing the aperture angle up to  $90^\circ$  and allowing a wider angular movement of the allen wrench.

The result of this modification was a better accessibility of the screws and a faster assembling of the columns.

During this first phase of support handling another problem emerged concerning the same sockets. As shown in figure [30](#) the wrench was not fitting in the sockets of the WPS column, because these were not long enough to host both the screw and the wrench. The same problem was affecting the HLS column, but as visible in figure [29](#) in that column it was possible to extend in height the socket, thanks to the bigger available space. For the WPS column it was impossible to implement further modifications, because the limited height of the support column was not allowing any other vertical extension of the socket.

The conclusions were that a shorter allen wrench will be used to fix the WPS support tube, while the HLS column sockets have been extended in height by 5 mm, simplifying the wrench access.

Another problem encountered in the tests was an interference between the allen wrench and the WPS column when fixing the height of the HLS sensor.

As shown in figure [31](#) with the WPS column already in place it was difficult to adjust the position of the HLS support tube, because the WPS installation was blocking the movement of the allen wrench. The risk was to touch and deteriorate the WPS sensor when adjusting the position of the HLS support tube. To solve this design issue the configuration of the holes to

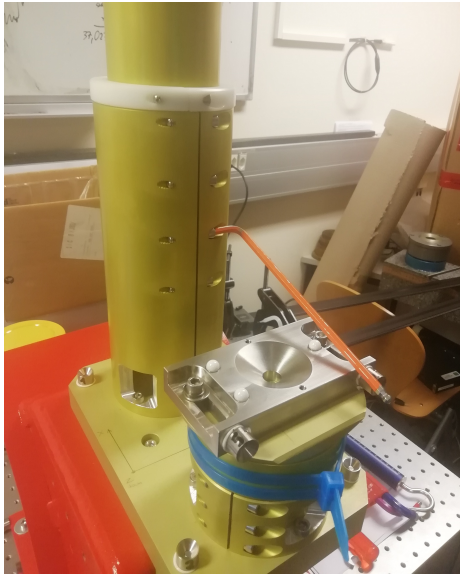


Figure 31: Wrench interference

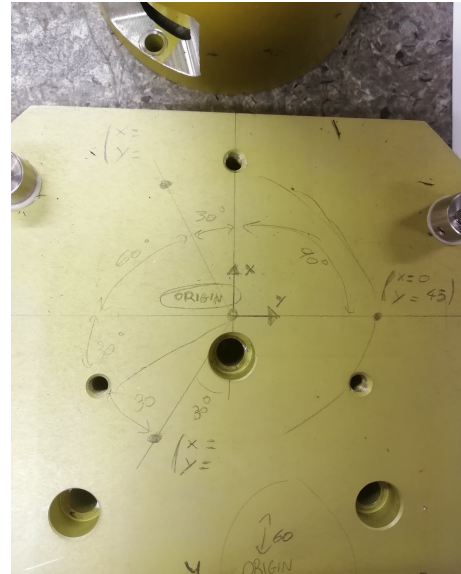


Figure 32: HLS holes orientation

fix the HLS column has been changed: a set of three new holes has been drilled on the support base, following the sketch in figure [32](#), to allow a rotation of the HLS column of  $90^\circ$ .

With the new position of the column the screws end up being on the side of the tube, where there is nothing blocking the movement of the wrenches.

This new orientation of the holes in the support plate has been updated and also the screws in the HLS support tube have been moved on the other side of the tube, so that in the final position the operator will fix the screws with the right hand.

### 5.3 Plastic stability

As described in section [4.3](#), the plastic stability is an important parameter for the sensor support. It is indeed fundamental for all the components connected to the sensors to resist any plastic deformation after an external force.

The aim of this third test series is to register and report any eventual plastic deformation of the sensor support after loading it with a certain lateral force.

The sensor support is not supposed to withstand lateral forces, but as reported the sensors and the rest of the equipment must be designed to face all possible situations.

This plastic stability test simulates the situation of someone using the sensor support to access above or behind the cryostat, by hanging on one of the two sensor support tubes. Similar situations occurred in the past with different supports, so the test has been conducted exactly like in the LHC environment, by using the sensor support as handle to climb the magnet.



The measurements of the deformation were calculated as difference between the initial and final position of the tubes:

- Measurement of the initial position of the sensor support tube, using the laser tracker with the target placed on top of the column in a live tracking mode.
- Pull the considered sensor support tube from the radial side by hanging on it, and then releasing the force.
- After some seconds, when the position of the system is stable, measure the new position and calculate the difference between the initial and the final position, to check the presence of any variation of the position values of the sensor with respect to the original ones.

This operation has been repeated for both WPS and HLS and using different extensions of the column along Z, to verify the influence of the extension of the sensor support tubes in the plastic deformation.

The tests have also been performed with two different configurations of the screws which hold the columns:

- With the use of all the screws (four in the HLS support tube and three for the WPS)
- With a reduced amount of the screws (two in the HLS tube and two in the WPS one)

This to verify the effective influence of the number of screws in the rigidity of the structure, and to see if the support was losing the fiducialisation when using only half of the screws. This test was important to consider the use of less screws for the final design of the sensor support. Using half of the screws could be an improvement for the ergonomics, as it allows faster installation and easier maintenance of the support, but it is important to avoid any risk of movement of the top tubes during all the years of HL-LHC operation, reason why some numerical values were needed to take the decision.

The outcome of the measurements is reported in tables [10](#) and [11](#), using the average of three iterations. The full length tables are reported in the appendix of the document, corresponding to tables [24](#) and [25](#).

Table 10: HLS plastic deformation

Config.	4 screws				2 screws			
	dx [ $\mu\text{m}$ ]	dy [ $\mu\text{m}$ ]	dz [ $\mu\text{m}$ ]	d3D [ $\mu\text{m}$ ]	dx [ $\mu\text{m}$ ]	dy [ $\mu\text{m}$ ]	dz [ $\mu\text{m}$ ]	d3D [ $\mu\text{m}$ ]
Bottom	-5	6	0	8	-8	9	1	12
Middle	-8	13	0	16	-7	4	6	11
High	-8	17	-1	20	2	-5	3	7

Table 11: WPS plastic deformation

Config.	3 screws				2 screws			
	dx [ $\mu\text{m}$ ]	dy [ $\mu\text{m}$ ]	dz [ $\mu\text{m}$ ]	d3D [ $\mu\text{m}$ ]	dx [ $\mu\text{m}$ ]	dy [ $\mu\text{m}$ ]	dz [ $\mu\text{m}$ ]	d3D [ $\mu\text{m}$ ]
Bottom	-	-	-	-	-1	-10	-3	11
High	-5	13	1	14	-19	5	1	19

In the tables above only the average values obtained from the three iterations are reported, the full length tables are table [24](#) and [25](#), reported in the appendix.

For the plastic stability the most relevant values are the movements along the Z and X axis, because these are the ones that influence more the sensors readings.

The obtained data demonstrates that no significant difference was detected between the two configurations. The deformation values were always close to the instrument precision in both cases and widely satisfying the requirements in terms of plastic stability, nevertheless the decision was to use all the screws in the final installation.

## 5.4 Elastic deformation resistance

The elastic deformation resistance of the support is intended as the capacity of the object to avoid elastic deformations when a force is applied.

This elastic resistance is of course not as important as the plastic stability, because it does not affect permanently the readings of the sensors and the shape of the support.

To examine the behaviour of the sensor support in terms of rigidity the test consisted in:

- Measuring the initial position of the system with the 1.5 inches sphere on top of the sensor support tube.

- Pulling with 20 kg force from one side of the support tube and holding the load.
- Measuring the reached deformation and release the applied load.

This process has been repeated applying the force along the X and Y axis, as shown in figure 33, using different heights of the columns and with the two different screw configurations. For each one of these combinations the described process has been performed three times, and the considered values were the average values of these three iterations.

All the data was collected in full-length tables that are reported in the appendix of the document in tables 26 to 29.

Since during the test the support was pulled along the X and Y axis the most interesting values of deformation are the ones along these two axis, indeed the deformation along Z was measured as almost zero, as illustrated in the following tables where the deformations along Z are therefore blurred in grey.



Figure 33: Pulling process configuration

Table 12: HLS elastic deformation 4 screws

Configuration		4 screws			
Position		dx [mm]	dy [mm]	dz [mm]	d3D [mm]
high	longitudinal	-0.022	-0.316	-0.009	0.317
	radial	-0.516	-0.043	-0.014	0.518
middle	longitudinal	-0.018	-0.222	-0.011	0.223
	radial	-0.363	-0.019	-0.008	0.364
low	longitudinal	-0.001	-0.156	-0.005	0.157
	radial	-0.250	-0.006	-0.005	0.251

Table 13: HLS elastic deformation 2 screws

Configuration		2 screws			
Position		dx [mm]	dy [mm]	dz [mm]	d3D [mm]
high	longitudinal	-0.049	-0.477	-0.011	0.479
	radial	-0.515	-0.032	-0.010	0.517
middle	longitudinal	-0.005	-0.184	-0.005	0.184
	radial	-0.281	-0.003	-0.003	0.281
low	longitudinal	0.019	-0.265	-0.007	0.266
	radial	-0.432	-0.049	-0.003	0.434

Table 14: WPS elastic deformation 3 screws

Configuration		3 screws			
Position		dx [mm]	dy [mm]	dz [mm]	d3D [mm]
high	longitudinal	-0.007	-0.019	-0.003	0.021
	radial	-0.041	0.002	-0.015	0.044
low	longitudinal	-0.020	-0.008	0.001	0.022
	radial	-0.034	-0.001	-0.011	0.036

Table 15: WPS elastic deformation 2 screws

Configuration		2 screws			
Position		dx [mm]	dy [mm]	dz [mm]	d3D [mm]
high	longitudinal	0.006	-0.017	0.004	0.018
	radial	-0.026	0.007	-0.009	0.029
low	longitudinal	-0.001	-0.013	-0.001	0.013
	radial	-0.042	-0.002	-0.016	0.045

The reported values are of course higher than the values of plastic deformation (Tables 10 and 11) because they do not consider the elastic comeback of the columns, but as anticipated the elastic deformation will not affect the sensors measurements critically, because after the load is released the final position of the sensor is almost the same as the original one.

As pointed out in the tables, the highest deformation has been recorded as around 500  $\mu\text{m}$  in the HLS tube when extended at its maximum position.

Considering that this value is along the radial axis and the influence along the Z axis is not significant, the overall rigidity of the support can be considered as satisfactory.

Also the difference between the use of all the screws or only half of them is not relevant in terms of elastic deformation, confirming the outcome of the plastic stability tests in section 5.3.

## 6 Conclusion

After the proposed modifications were implemented, the prototype of the sensor support met the requirements described in section 4 in every aspect that has been tested.

The adjustment range along Z of the HLS and WPS columns was comfortably wider than the required, but to comply with the wire sag and with the HLS steps along the 200 m long tunnel it will be necessary to have different configurations of the sensor support, with bottom tubes of different length depending of the area of the tunnel where the support will be installed.

For the rotations of the tilt lenses, the adjustment range was also larger than the required, nevertheless it was necessary to use grease on the contact surfaces of the tilt lenses, to be able to adjust the inclinations with enough precision and reach the extremities of the range.

The adopted grease was the Petamo GHY 133N, which is a radiation resistant lube. Since during its operation the support will be subjected to high level of radiation it is necessary to use radiation resistant lube, to avoid the degradation of the grease along the time, which could bring the two surfaces to stick together and making it impossible to move again the lenses.

The minor issues concerning the dimension of the washers have been solved by modifying the dimension of the socket where the washers fit. The dimension of the socket has indeed been increased in width of 1 mm in the plans, so that the standardized M8 washer will fit perfectly in the last version of the sensor support.

The ergonomics of the sensor support was one of the most important parameters to be tested, as the support will be partially assembled by hand and installed in the tunnel, where the available space is limited and the time slots to perform each operation have to be organized to make the most of the limited time.

The overall evaluation of the sensor support in terms of ergonomics is positive, and with the tests some problems have been identified and corrected.

For the safety aspects, the only note is concerning the potentially dangerous accidental drop of the HLS column, which was experienced while handling the support during the tests, as described in section 5.1.1. To reduce the risk of damaging the equipment and injuring the operators a safety device was needed, and the idea was to use a ring to block the tube from suddenly falling down. Two designs are proposed: a simpler one with an one screw closure system and a more ergonomic one with a clamp to fix the position of the ring along the tube. These two versions are presented in figures 23 and 24.

Every modification of the prototype was made with the purpose of reducing the assembling

time and make the assembling process as fast as possible, for example the modifications to the sockets where to fit the allen wrenches, that have been widened to allow wider rotations of the wrenches and in the case of HLS also the possibility to fit normal size wrenches.

The required time to assemble the sensor support and all its components was roughly 7 minutes, but this time has to be combined with the needed time to adjust the position of the sensors, which is shown in tables [22](#) and [23](#), resulting in an overall time of 10 to 15 minutes. To optimize even further the time spent in the tunnel to assemble the support it is possible to pre-assemble the columns and fix in a provisional position the tilt lenses.

Some modifications were implemented in the design of the support, like the tolerance of the tubes, that have been modified to be sure that in none of the roughly 200 supports that will be produced there will be any kind of undesired interference in between the components. Nevertheless each assembly will be checked for compliance before the installation.

The modifications to the screw sockets of the support tubes have been integrated, and also the holes configuration in the support base has been changed for the HLS support tube, to have the column in a comfortable position during the assembling process, avoiding any interference of the wrenches with the equipment in the proximity. The position on the screw in the HLS support tube has been mirrored in the other side of the component, to ensure their accessibility. The behaviour of the sensor support under load was excellent, both from the plastic stability and elastic deformation resistance point of view. All the deformation values registered during the tests were compliant with the needs, with a maximum plastic deformation of 17  $\mu\text{m}$  for HLS along Y and 19  $\mu\text{m}$  along X for WPS.

In terms of elastic deformation, less critical than the plastic one, the highest reached values were 500  $\mu\text{m}$  for the HLS along X in its maximum extension, and less than 50  $\mu\text{m}$  for the WPS support along X.

These results are more than satisfying, considering that one of the most critical deformations is along the Z axis, where the reported plastic deformations are almost zero and the elastic deformations are below 15  $\mu\text{m}$ .

From the tests with half of the screws emerged that both for the rigidity and the stability no substantial difference was found, but the final decision was to support the safest option of using all the screws in the HLS and WPS column.

The prototype has been validated and is ready for the pre-series production. The final version of the support will then be ready to be installed in the tunnel for the operation of HL-LHC.

## References

- [1] CERN (internal), *Internal reports*  
<https://edms.cern.ch/ui/#!master/navigator/document?D:100870900:100870900:subDocs> (20.09.2021)
  - [2] CERN, *Official website*  
<https://home.cern/> (30.08.2021)
  - [3] CERN, *Our people*  
<https://home.cern/about/who-we-are/our-people> (18.09.2021)
  - [4] CERN, *CERN's timeline*  
<https://home.cern/about/who-we-are/our-history> (27.09.2021)
  - [5] CERN, *Accelerator complex*  
<https://home.cern/science/accelerators/accelerator-complex/panoramas>  
(17.09.2021)
  - [6] CERN, *European Strategy for Particle Physics*  
<https://home.cern/news/news/cern/cern-council-updates-european-strategy-particle-physics> (16.09.2021)
  - [7] CERN, *LHC schedule*  
<https://home.cern/news/news/accelerators/new-schedule-lhc-and-its-successor> (16.09.2021)
  - [8] CERN, *Document server*  
<https://cds.cern.ch/record/2743293?ln=it> (20.10.2021)
  - [9] CERN, *CERN safety code*  
[https://edms.cern.ch/ui/file/335729/LAST\\_RELEASED/F\\_E.PDF](https://edms.cern.ch/ui/file/335729/LAST_RELEASED/F_E.PDF) (17.09.2021)
  - [10] World nuclear association, *Radiation exposure examples*  
<https://world-nuclear.org/information-library/safety-and-security/radiation-and-health/nuclear-radiation-and-health-effects.aspx> (17.09.2021)
  - [11] CERN (internal), *Fluka simulation*  
<https://edms.cern.ch/ui/#!master/navigator/document?D:100673477:100673477:subDocs> (17.09.2021)
  - [12] CERN (internal), *Fluka simulation*  
<https://edms.cern.ch/ui/#!master/navigator/document?D:100673477:100673477:subDocs> (17.09.2021)
-



- [13] CERN (internal), *3D model*  
<https://edms.cern.ch/ui/#!master/navigator/document?D:100859799:100859799:subDocs> (17.09.2021)
- [14] CERN (internal), *3D model*  
<https://edms.cern.ch/ui/#!master/navigator/document?D:100575456:100575456:subDocs> (17.09.2021)
- [15] CERN, *3D model*  
[https://indico.cern.ch/event/831552/contributions/3484751/attachments/1896045/3131761/2019-08-27\\_WP15\\_integration.pptx](https://indico.cern.ch/event/831552/contributions/3484751/attachments/1896045/3131761/2019-08-27_WP15_integration.pptx) (17.09.2021)
- [16] CERN (internal), *3D model*  
[https://edms.cern.ch/file/2606210/1/201\\_MS\\_wps\\_inhouse.pptx](https://edms.cern.ch/file/2606210/1/201_MS_wps_inhouse.pptx) (17.09.2021)
- [17] CERN (internal), *3D model*  
[https://edms.cern.ch/file/2606210/1/103\\_MS\\_hls\\_fsi.pptx](https://edms.cern.ch/file/2606210/1/103_MS_hls_fsi.pptx) (17.09.2021)
- [18] CERN (internal), *Functional specification*  
<https://edms.cern.ch/ui/#!master/navigator/document?D:100720110:100720110:subDocs> (17.09.2021)
- [19] CERN (internal), *Wire sag*  
<https://edms.cern.ch/document/2117098/1> (20.10.2021)
- [20] CERN, *Material choice*  
[https://edms.cern.ch/ui/file/335806/LAST\\_RELEASED/IS41\\_E.pdf](https://edms.cern.ch/ui/file/335806/LAST_RELEASED/IS41_E.pdf) (20.09.2021)
- [21] CERN, *Actiwiz*  
<https://actiwiz-dev.web.cern.ch/> (17.09.2021)
-

## 7 Appendix

Table 16: HLS rotations around X

	+ [mrad]	- [mrad]	range [mrad]	range [deg]
Pos 1	52.980	41.920	94.900	5.44
	52.710	44.370	97.080	5.56
	54.290	47.610	101.900	5.84
Pos 2	40.810	54.400	95.210	5.46
	42.775	53.220	95.995	5.50
	40.960	54.200	95.160	5.45

Table 17: HLS rotations around Y

	+ [mrad]	- [mrad]	range [mrad]	range [deg]
Pos 1	36.675	12.810	49.485	2.84
	36.760	13.360	50.120	2.87
	36.650	16.340	52.990	3.04
Pos 2	13.045	36.450	49.495	2.84
	13.220	36.065	49.285	2.82
	12.870	36.160	49.030	2.81

Table 18: WPS rotations around X

	+ [mrad]	- [mrad]	range [mrad]	range [deg]
Pos 1	51.830	49.340	101.170	5.80
	52.750	48.000	100.750	5.77
	53.070	49.370	102.440	5.87
Pos 2	48.915	51.415	100.330	5.75
	49.225	53.495	102.720	5.89
	47.640	53.535	101.175	5.80

---

Table 19: WPS rotations around Y

	+ [mrad]	- [mrad]	range [mrad]	range [deg]
Pos 1	33.650	16.995	50.645	2.90
	33.660	16.540	50.200	2.88
	34.140	16.100	50.240	2.88
Pos 2	16.800	34.140	50.940	2.92
	15.605	33.980	49.585	2.84
	15.330	33.790	49.120	2.81

Table 20: WPS rotations Z tilt lenses

Iterations	+	-	delta [mrad]	delta [deg]
1	374.100	466.793	92.693	5.311
2	375.768	467.550	91.782	5.259
3	374.352	464.449	90.097	5.162
Average:			91.524	5.244

Table 21: WPS rotations Z 3 ball interface

Iterations	+	-	delta [mrad]	delta [deg]
1	229.445	714.283	484.838	27.779
2	229.602	721.136	491.534	28.163
3	225.978	720.403	494.425	28.328
Average:			490.266	28.090

---

Table 22: HLS ergonomics

HLS							
iteration	feature	unit	Tz	Rx	Ry	total time	operator
1	residual	[ $\mu\text{m}$ ] [ $\mu\text{rad}$ ]	18	255	780	02:45	A
	time	[mm:ss]	01:15	02:45	02:45		
2	residual	[ $\mu\text{m}$ ] [ $\mu\text{rad}$ ]	35	340	550	02:00	A
	time	[mm:ss]	00:45	02:00	02:00		
3	residual	[ $\mu\text{m}$ ] [ $\mu\text{rad}$ ]	50	2275	1100	03:10	B
	time	[mm:ss]	01:40	03:10	03:10		
4	residual	[ $\mu\text{m}$ ] [ $\mu\text{rad}$ ]	45	110	50	02:55	B
	time	[mm:ss]	01:20	02:55	02:55		
5	residual	[ $\mu\text{m}$ ] [ $\mu\text{rad}$ ]	15	2720	1150	05:14	B
	time	[mm:ss]	01:10	05:14	05:14		

Table 23: WPS ergonomics

WPS									
iteration	feature	unit	Tz	Rx	Ry	Tx	Rz	total time	operator
1	residual	[ $\mu\text{m}$ ] [ $\mu\text{rad}$ ]	30	255	780	50	3000	07:45	B
	time	[mm:ss]	01:20	02:45	02:45	07:45	07:45		
2	residual	[ $\mu\text{m}$ ] [ $\mu\text{rad}$ ]	100	1050	1975	10	422	08:05	A
	time	[mm:ss]	01:15	02:30	02:30	08:05	08:05		
3	residual	[ $\mu\text{m}$ ] [ $\mu\text{rad}$ ]	60	710	1790	30	50	06:30	A
	time	[mm:ss]	01:30	02:30	02:30	06:30	06:30		
4	residual	[ $\mu\text{m}$ ] [ $\mu\text{rad}$ ]	82	270	1090	146	322	09:05	B
	time	[mm:ss]	03:04	04:47	04:47	09:05	09:05		
5	residual	[ $\mu\text{m}$ ] [ $\mu\text{rad}$ ]	60	1280	500	30	380	05:54	B
	time	[mm:ss]	01:20	02:45	02:45	05:54	05:54		

Table 24: Plastic stability - HLS - extended table

		HLS						
Config.	4 screws				2 screws			
Position	dx [ $\mu\text{m}$ ]	dy [ $\mu\text{m}$ ]	dz [ $\mu\text{m}$ ]	d3D [ $\mu\text{m}$ ]	dx [ $\mu\text{m}$ ]	dy [ $\mu\text{m}$ ]	dz [ $\mu\text{m}$ ]	d3D [ $\mu\text{m}$ ]
bottom	-4	6	-1	7	-5	8	-1	10
	-3	8	3	9	-9	11	2	14
	-7	5	-3	9	-10	7	1	12
middle	-7	14	-5	16	-7	4	4	9
	-12	15	3	19	-4	-2	8	9
	-4	11	1	12	-9	9	6	14
high	-12	20	-1	23	3	-7	2	8
	-3	13	3	14	1	-5	4	7
	-9	18	-6	22	3	-3	2	5

Table 25: Plastic stability - WPS - extended table

		WPS						
Config.	3 screws				2 screws			
Position	dx [ $\mu\text{m}$ ]	dy [ $\mu\text{m}$ ]	dz [ $\mu\text{m}$ ]	d3D [ $\mu\text{m}$ ]	dx [ $\mu\text{m}$ ]	dy [ $\mu\text{m}$ ]	dz [ $\mu\text{m}$ ]	d3D [ $\mu\text{m}$ ]
bottom	-	-	-	-	-1	-10	-5	11
	-	-	-	-	-4	-11	-5	13
	-	-	-	-	1	-9	2	9
high	-3	9	2	9	-15	4	1	15
	-8	25	-2	26	-19	9	4	21
	-4	5	2	7	-22	3	-1	22

Table 26: Elastic rigidity - HLS - extended table - 4 screws

HLS					
Configuration		4 screws			
Position		dx [mm]	dy [mm]	dz [mm]	d3D [mm]
high	longitudinal	-0.016	-0.319	-0.008	0.320
		-0.023	-0.302	-0.009	0.303
		-0.028	-0.327	-0.010	0.328
	radial	-0.504	-0.052	-0.016	0.507
		-0.519	-0.038	-0.012	0.521
		-0.524	-0.038	-0.014	0.526
middle	longitudinal	0.006	-0.214	-0.012	0.214
		-0.039	-0.213	-0.010	0.217
		-0.020	-0.238	-0.010	0.239
	radial	-0.374	0.001	-0.012	0.374
		-0.370	-0.021	-0.009	0.371
		-0.346	-0.038	-0.004	0.348
low	longitudinal	0.000	-0.168	-0.007	0.168
		-0.013	-0.145	-0.005	0.146
		0.009	-0.156	-0.004	0.156
	radial	-0.250	-0.012	-0.004	0.250
		-0.240	0.001	-0.005	0.240
		-0.261	-0.008	-0.006	0.261

Table 27: Elastic rigidity - HLS - extended table - 2 screws

HLS					
Configuration		2 screws			
Position		dx [mm]	dy [mm]	dz [mm]	d3D [mm]
high	longitudinal	-0.060	-0.471	-0.009	0.475
		-0.045	-0.479	-0.014	0.481
		-0.043	-0.480	-0.011	0.482
	radial	-0.527	-0.045	-0.012	0.529
		-0.517	-0.040	-0.010	0.519
		-0.502	-0.010	-0.007	0.502
middle	longitudinal	-0.007	-0.182	-0.006	0.182
		-0.008	-0.187	-0.006	0.187
		-0.001	-0.183	-0.004	0.183
	radial	-0.294	-0.005	-0.004	0.294
		-0.278	-0.007	-0.001	0.278
		-0.271	0.003	-0.004	0.271
low	longitudinal	0.023	-0.255	-0.007	0.256
		0.019	-0.275	-0.008	0.276
		0.014	-0.266	-0.007	0.266
	radial	-0.418	-0.046	-0.003	0.421
		-0.446	-0.047	-0.005	0.448
		-0.431	-0.053	-0.001	0.434

Table 28: Elastic rigidity - WPS - extended table - 3 screws

WPS					
Configuration		3 screws			
Position		dx [mm]	dy [mm]	dz [mm]	d3D [mm]
high	longitudinal	-0.003	-0.018	-0.004	0.019
		-0.010	-0.020	-0.003	0.023
		-0.007	-0.020	-0.003	0.021
	radial	-0.036	0.000	-0.015	0.039
		-0.041	0.002	-0.017	0.044
		-0.047	0.004	-0.014	0.049
low	longitudinal	-0.023	-0.008	0.001	0.024
		-0.017	-0.008	0.000	0.019
		-0.020	-0.009	0.001	0.022
	radial	-0.034	-0.003	-0.012	0.036
		-0.035	-0.001	-0.010	0.036
		-0.034	0.000	-0.012	0.036



Table 29: Elastic rigidity - WPS - extended table - 2 screws

WPS					
Configuration		2 screws			
Position		dx [mm]	dy [mm]	dz [mm]	d3D [mm]
high	longitudinal	0.002	-0.018	0.005	0.019
		0.009	-0.015	0.002	0.018
		0.007	-0.017	0.005	0.019
	radial	-0.026	0.005	-0.009	0.028
		-0.030	0.008	-0.011	0.033
		-0.022	0.009	-0.007	0.025
low	longitudinal	-0.001	-0.011	-0.006	0.013
		-0.002	-0.009	0.000	0.009
		-0.001	-0.018	0.002	0.018
	radial	-0.043	-0.002	-0.018	0.047
		-0.039	-0.002	-0.015	0.042
		-0.044	-0.002	-0.014	0.046